Time-Resolved Dynamic Light Scattering Studies on Gelation Process of Organic−Inorganic Polymer Hybrids

Tomohisa Norisuye and Mitsuhiro Shibayama*

Department of Polymer Science and Engineering, Kyoto Institute of Technology, Matsugasaki, Sakyo-ku, Kyoto 606-8585, Japan

Ryo Tamaki and Yoshiki Chujo

Department of Polymer Chemistry, Graduate School of Engineering, Kyoto University, Yoshida, Sakyo-ku, Kyoto 606-8501, Japan

Received August 18, 1998; Revised Manuscript Received January 12, 1999

ABSTRACT: The gelation process of organic−inorganic polymer hybrids has been investigated by time-resolved dynamic light scattering. The polymer hybrids were prepared by sol−gel reaction of tetramethoxysilane (TMOS) in the presence of organic compounds, such as poly(dimethylacrylamide) (poly-DMAA) or DMAA monomers. The gelation threshold was characterized by (1) the drastic change in the scattered intensity and an appearance of a speckle pattern during the course of gelation, (2) a power-law behavior of the time−intensity correlation function (ICF), $g^{(2)}(\tau) - 1$, where τ is the decay time, (3) the appearance of a long tail in the characteristic decay time distribution function, and (4) the reduction of the initial amplitude of ICF. The gelation process of TMOS was found to be strongly dependent on the presence of either poly-DMAA or DMAA monomers. In the presence of poly-DMAA, the gelation was accelerated. On the other hand, it was decelerated when DMAA monomers were present in the system. On the basis of this experimental evidence, we concluded that hydrogen bonding between the amide groups in DMAA and silanol groups in TMOS plays an important role in the gelation kinetics of these hybrids.

1. Introduction

Organic−inorganic polymer hybrids have recently been synthesized by the so-called sol−gel method of alkoxysilanes.[1,2] The sol−gel reaction comprises hydrolysis and subsequent condensation reaction of alkoxy- or hydroxysilanes as shown in Scheme 1. When alkoxysilanes are used as precursors, Si−OH groups are formed by hydrolysis of alkoxy groups (step 1). Subsequent condensation of the hydroxyl groups leads to a formation of a Si−O−Si linkage (step 2). With further hydrolysis and condensation, a siloxane network develops via cross-linking of the oligomers (step 3). Among a variety of polymer hybrids, it has been reported that organic−inorganic hybrid polymers consisting of poly(2-methyl-2-oxazoline),[3,4] poly(*N*-vinylpyrrolidone),[5] or poly(*N*,*N*-dimethyl acrylamide) (DMAA)[6] with these inorganic components are homogeneous and transparent over a wide range of compositions. Interestingly, the organic component was found to be molecularly dispersed in a silica matrix in most cases. The origin of the molecular-order miscibility is due to hydrogen bonding between the amide groups in the organic monomers and the silanol groups in the inorganic component. This sol−gel method, therefore, readily leads to potential applications of these hybrids for optical devices, such as optical waveguides,[7] optical biosensors,[8] etc. Recently, Tamaki et al. reported a novel method for preparing a hybrid gel of DMAA with tetramethoxysilane (TMOS) by an in-situ radical polymerization.[6] This allows one to obtain homogeneous and transparent materials with good mechanical properties and advanced temperature resistance.

Polymer hybrids contain more than two components, i.e., organic and inorganic constituents as well as solvent. Therefore, due to its complexity, the kinetics of sol−gel reaction has not been well elucidated. In the case of rather simpler systems comprising solely either organic or inorganic component, many researchers have reported several methods to determine the gelation threshold. For example, according to Winter et al., dynamic viscoelastic measurements provide accurate determination of the gelation point.[9−11] Martin et al. showed a power-law behavior in the structure factor obtained by small-angle X-ray (SAXS) and/or neutron scattering (SANS) for a system just below the gelation threshold.[12−15] However, these methods have some disadvantages: For instance, the gelation threshold cannot be determined without mechanical disturbance in the case of dynamic viscoelastic measurements. SAXS and SANS are, in most cases, irrelevant for a real time measurement of gelation because of low counting rates. Particularly, sol−gel reaction of polymer hybrids is more intricate due to the following reasons: (1) They are multicomponent systems. (2) A complicated chemistry, such as hydrolysis and condensation, is involved. (3) Glassy materials are formed after gelation, which means formation of a nonequilibrated or frozen structure.

To characterize the gelation kinetics of polymer hybrids by circumventing these difficulties, we have developed a novel method to elucidate the gelation mechanism and gelation threshold. In the previous

Scheme 1

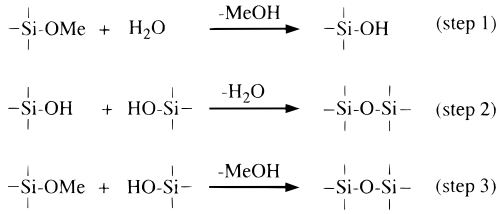

* To whom correspondence should be addressed.

10.1021/ma981306h CCC: $18.00
Published on Web 02/12/1999

paper, we demonstrated that light scattered intensity is very sensitive to the gelation threshold provided the system is transparent throughout the gelation process.[16] In this paper, we deeply take into account the nature of cross-linked polymer chain clusters near the gelation threshold and propose a multiaspect method for the determination of gelation threshold. First of all, we propose four methods for determination of the gelation threshold by time-resolved dynamic light scattering (TRDLS), which are characterized by (1) a drastic change in the scattered intensity and an appearance of the speckle pattern during the course of gelation, (2) a power-law behavior of the time intensity correlation function (ICF), $g^{(2)}(\tau) - 1$, where τ is the decay time, (3) an appearance of a long tail in the characteristic decay time distribution function, and (4) a reduction of the initial amplitude of ICF. Regarding (2), the fact that a power law appears was already reported by Martin and Wilcoxon,[14] Lang and Buchard,[17] and Ren and Sorensen.[18] However, the methods proposed in this work are more persuasive because each method is strongly supported by the physics of gels, i.e., nonergodicity and/or self-similarity. The feasibility of these four methods will be examined on a gelation of TMOS. Second, the dynamics of chain clusters near the gelation threshold will be discussed on the basis of percolation model. Finally, the methods proposed for the determination of the gelation threshold will be applied for investigation of the gelation kinetics of DMAA/TMOS polymer hybrids, where effects of DMAA monomers or polymers present in the reaction bath will be discussed.

2. Experimental Section

2.1. Samples. Tetramethoxysilane (TMOS) and dimethylacrylamide (DMAA) were purified by distillation under nitrogen. DMAA polymers (poly-DMAA) were prepared by radical polymerization with azobis(isobutyronitrile) (AIBN) as initiator in advance to preparing hybrids. AIBN was recrystalized prior to the use. The samples for DLS measurements were prepared as follows: Prescribed amounts of TMOS monomers and DMAA monomers or poly-DMAA were dissolved in 9 mL of dimethylformamide (DMF) in a 10 mm diameter test tube at room temperature under N_2 purge. The polymer concentration was fixed to be 10 wt % for the case of the TMOS system. In the case of the TMOS/DMAA system, the concentrations were set to be 5 wt % each. The details of the sample preparation method are described elsewhere.[6] In addition to the TMOS/DMAA, TMOS−styrene monomer and TMOS−polystyrene hybrids were also prepared to confirm the effect of hydrogen bonding present in the TMOS/DMAA. The concentrations of styrene monomers and polystyrene were also chosen to be 5 wt % each.

2.2. Dynamic Light Scattering. Time-resolved dynamic light scattering (TRDLS) measurements were carried out on a DLS/SLS-5000 compact goniometer, ALV, Langen, coupled with an ALV photon correlator. The polymerization/gelation of the samples described above was initiated by adding 0.236 mL of 1 N HCl (catalyst) just before DLS measurements, and the DLS measurements were carried out at 58 °C as a function of polymerization time, t. A 35 mW helium−neon laser (the wavelength in a vacuum; $\lambda = 632.8$ nm) was used as the light source. Scattered intensity data were collected as a function of the polymerization time, t, during about 70 h of reaction, from which the intensity time correlation function, $g^{(2)}(\tau)$, was calculated in a wide range of logarithmic lag time scale, log τ. The acquisition time for each run was 500 s. The characteristic decay time distribution function, $P(\Gamma^{-1})$, was obtained from $g^{(2)}(\tau)$ with an inverse Laplace transform program (a constrained regularization program, CONTIN provided by ALV).

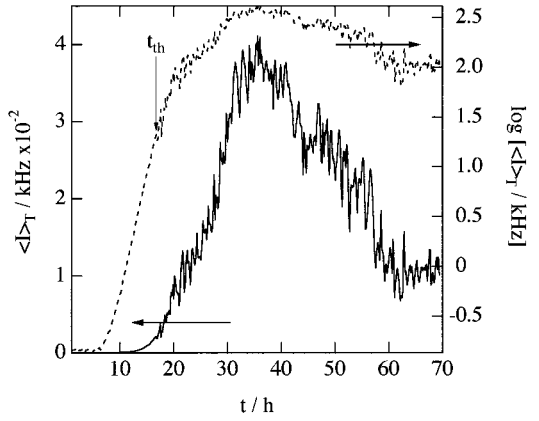

Figure 1. Evolution of the scattered intensity, $\langle I\rangle_T$, during polymerization of TMOS: linear plot (solid line) and logarithmic plot (dashed line). t_{th} denotes the gelation threshold.

3. Results and Discussion

3.1. Determination of Gelation Threshold by TRDLS. Figure 1 shows the scattered intensity variation of TMOS as a function of polymerization time t, where $\langle I\rangle_T$ denotes the time average scattered intensity observed at the scattering angle of 90°. The dashed line shows log[$\langle I\rangle_T$], which emphasizes the onset of the steep increase in $\langle I\rangle_T$ with time. As shown in the figure, the scattered intensity is quite low for $t < 6$ h, suggesting no reaction occurred in the system. However, for $6 < t < 17$ h, the intensity gradually increased as a result of a growth of poly-TMOS clusters. For $t > t_{th} \approx 17$ h, the intensity began to show strong fluctuations in $\langle I\rangle_T$, which is due to the nonergodic nature of gels, in other words, an appearance of frozen inhomogeneities by cross-links.[19−21] We believe that this point corresponds to the gelation threshold according to our previous work.[22] At this point, finite clusters start to connect each other. The cross-link effect seems to be still weak at the gelation threshold. This is why the subsequent increase in $\langle I\rangle_T$ takes place. This means that the gelation still continues until "space filling" by poly-TMOS clusters attains. The space filling here means that the envelopes of the clusters fill the space. After the space filling, attained around $t = 30$ h, $\langle I\rangle_T$ gradually decreases with strong fluctuations. This decrease in $\langle I\rangle_T$ results from a reduction of the difference in the refractive index due to depletion of the solvent phase. A similar behavior in $\langle I\rangle_T$ was observed in an organic system, e.g., gelation of acrylamide gels by redox polymerization, as far as the gelation starts from a monomer solution.[22]

Figure 2 shows the double-logarithmic plot of the intensity time correlation functions (ICF) during gelation. In the beginning ($t < 10$ h), the scattered photons are too few to build an ICF. However, for $t > 7$ h, the ICF shows a characteristic decay time at $\tau \sim 10^{-2}$ ms. At $t \sim 17$ h, the ICF has a long tail at the larger value of τ. At this point, the ICF seems to be well described with a power law function. This corresponds to the gelation threshold as stated above. Martin et al. reported that the ICF at the gelation threshold is given by a sum of two contributions, i.e., a diffusive mode and a power-law behavior, as follows[15]

$$g^{(2)}(\tau) - 1 = [A \exp[-\Gamma_{fast}\tau] + (1 - A)(1 + \tau/\tau^*)^{-(1-D_P)/2}]^2 \quad (1)$$

where Γ_{fast} and τ^* are a characteristic decay rate of the

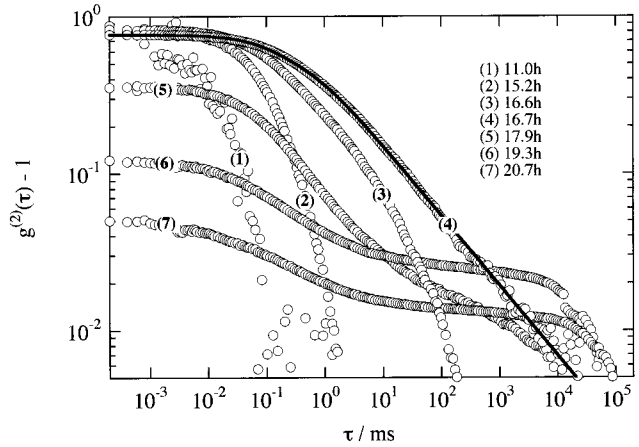

Figure 2. Double-logarithmic plots of the intensity time correlation functions (ICFs) during polymerization of TMOS. The solid line on curve 4 indicates the result of curve fit with eq 1.

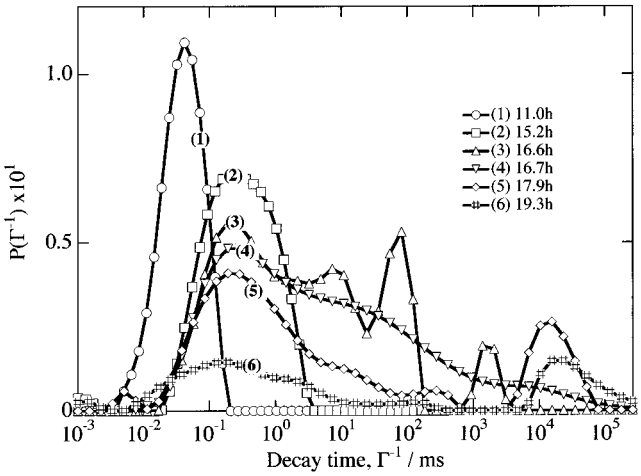

Figure 3. Decay time distribution functions $P(\Gamma^{-1})$ for TMOS during polymerization.

fast (diffusive) mode and a characteristic decay time above which a power-law behavior appears. D_p is the fractal dimension of the scattered photons. A ($0 \leq A \leq 1$) is the relative strength of the diffusive mode. The solid line on the curve 4 in Figure 2 was obtained by fitting ICF with eq 1 to the case of $t \sim 17$ h. This fit gives $D_p = 0.53 \pm 0.1$. A further discussion on the scaling exponent will be given in the next section. For $t > 17$ h, the value of $[g^{(2)}(\tau \rightarrow 0) - 1]$ becomes much lower than unity due to the nonergodicity of the gel.

The characteristic decay time distribution function, $P(\Gamma^{-1})$, can be employed to discuss the characteristic behavior of ICF. $P(\Gamma^{-1})$ is obtained by inverse Laplace transform using a constrained regularization program, CONTIN, as follows

$$g^{(2)}(\tau) - 1 = [\int_0^\infty G(\Gamma) \exp(-\Gamma\tau)\, d\Gamma]^2 \qquad (2)$$

where Γ is the characteristic decay rate (an inverse of the characteristic decay time, Γ^{-1}). We define the characteristic decay time distribution function being $P(\Gamma^{-1}) \equiv G(\Gamma)$ for convenience.

Figure 3 shows the time variation of $P(\Gamma^{-1})$ for silica gels during gelation. For $t \sim 11$ h, a unimodal distribution of $P(\Gamma^{-1})$ is observed. This unimodal peak becomes broader and shifts to the longer relaxation time as the polymerization goes on. The peak is broadest around

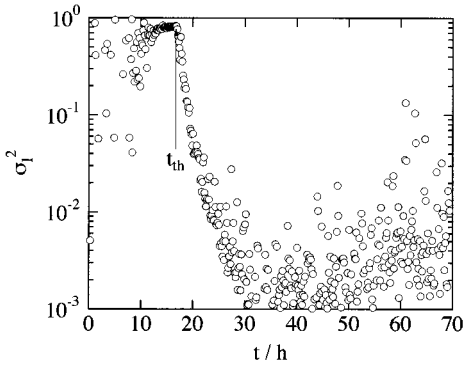

Figure 4. Time variation of the initial amplitude of ICF, σ_I^2, for TMOS during polymerization. t_{th} denotes the gelation threshold.

17 h (numbered to 4) where the gelation threshold is located. It should be noted here that a number of peaks in curves 3 and 5 seem to be an artifact by CONTIN, and they are not related to any specific size of clusters.

For $t \geq 17$ h, the distribution becomes narrower again. In the case of poly(*N*-isopropylacrylamide) (NIPA) gel, $P(\Gamma^{-1})$ was reduced to a pulselike function for $t \gg t_{th}$.[23] This means that the ICF is simply described by a single-exponential function, the so-called gel mode.[24] However, the well-developed silica gel obtained at $t \sim 19$ h does not show such a clear gel mode. On the other hand, Martin et al. also reported that the silica gel shows a power-law behavior in ICF even in the well-developed gels.[15] One of the reasons why two types of ICFs are present may be due to the difference of the degree of branching between the two systems—higher (TMOS) and lower (NIPA gels), as will be discussed in section 3.2. It should be also noted that the silica gels employed by Martin et al.[15] were prepared by NH_3OH base catalyst, which leads to highly branched silica gels compared to the ones used in this work (acid base). Therefore, the degree of branching can be ranked as follows: TMOS gels (base catalyst) > TMOS gels (acid catalyst) > NIPA gels.

Figure 4 shows the polymerization time, t, dependence of the initial amplitude of ICF, σ_I^2, for TMOS. As shown in the figure, σ_I^2 drops at $t \sim 17$ h. This is ascribed to the fact that the nonergodic nature appears when an infinite cluster, i.e., a gel, is formed.[21,23] However, for $t > 17$ h, σ_I^2 tends to be a decreasing function of t until the structure is stable. These four methods discussed above give the same result on the gelation threshold. In the case of the gelation process of TMOS above 5 wt %, the gelation threshold, t_{th}, was determined as $t_{th} = 17$ h.

3.2. Percolation Dynamics. As has been extensively discussed in the literature,[25,26] the percolation model has very strong implications on the static properties of branched polymer clusters near the gelation threshold, such as the fractal geometry and the mass distribution law. To examine the connectivity of the branched polymer systems, however, it is more essential to study the transport properties, such as rheological properties or chain dynamics.

According to Winter et al., the shear modulus has a power law dependence on ω at the gelation threshold[10]

$$G' \sim G'' \sim \omega^u \qquad (3)$$

where G' and G'' are the storage and loss moduli, respectively. They obtained $u \approx 1/2$ for poly(dimethylsi-

loxane). However, significantly different values for u ($\approx$0.7) were reported for branched polymers consisting of rather short strands.[14,27] According to Winter et al., this discrepancy is due to the architecture of the clusters, i.e., the ratio of the bifunctional and tetrafunctional (cross-linker) monomer groups.[11] They obtained the u value ranging from $^1/_2$ to $^2/_3$ by varying the ratio. Muthukumar explained the value of u from the viewpoints of polydispersity and the screening effect of excluded volume.[28] According to the theory, u is given by

$$u = \frac{\bar{D}}{\bar{D} + 2} \quad \text{(for a monodisperse semidilute solution)} \quad (4)$$

where $\bar{D}$ is the fractal dimension where the excluded-volume effect is neglected. Since $\bar{D}$= 2 for linear polymers, u is obtained to be $^1/_2$ for *slightly* cross-linked networks. On the other hand, polydisperse branched chain clusters comprising relatively short strands can be described by the percolation model

$$u = \frac{d}{D + 2} \quad \text{(polydisperse chain clusters)} \quad (5)$$

where d and D are the space dimension and the fractal dimension in the presence of excluded-volume interaction, respectively. The hyperscaling hypothesis gives the relationship between D and the Fisher's exponent for polydispersity, τ_F

$$\tau_F - 1 = \frac{d}{D} \quad (6)$$

Thus, $D = {}^5/_2$ is obtained by substituting $d = 3$ and $\tau_F \approx 2.2$ (percolation theory), which leads to $u = {}^2/_3$. This may be the case reported by Durand et al.[27] and Martin et al.[15]

The discussion given above is important to elucidate the nature of the observed exponent D_p by DLS, since D_p is equal to u.[26] As already shown in the previous section, the evaluated value of D_p in the TMOS clusters was around 0.53 $\pm$ 0.1, which is significantly smaller than the value reported by Martin and co-workers, e.g., D_p = 0.73 for silica gels.[15] This is ascribed to the difference in the preparation method of silica gels. They used a base catalyst to obtain silica gels, which resulted in a highly branched silica gels. On the other hand, our gel was prepared with an acidic catalyst. It is reported that an acidic catalyst leads to a relatively long silica chains between cross-links.[29] Note that we also obtained D_p = 0.84 $\pm$ 0.1 for silica gels prepared with a base catalyst (ammonium hydroxide).

In any case, it can be concluded that the TMOS clusters near the gelation threshold can be described by percolation theory. The exponent obtained in the gels studied here indicates that the system is rather close to the one studied by Winter ($u \approx 0.5$), i.e., long-chain network with a small ratio of cross-linking. This problem is related to the degree of branching as discussed above.

3.3. Gelation Process of Organic−Inorganic Hybrid Polymer Gels. In this section, we apply the above four methods to various types of polymer hybrids. It will be demonstrated that these methods make clear the effects of the presence of organic components on the gelation of polymer hybrids.

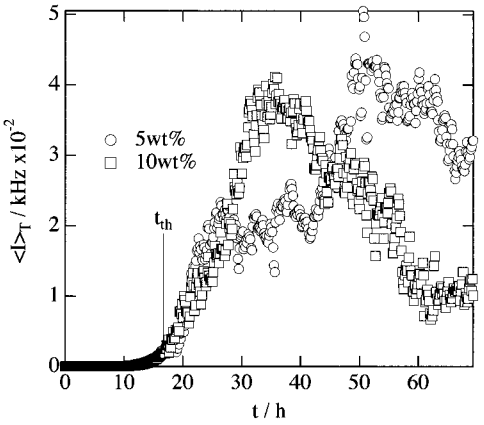

Figure 5. TMOS monomer concentration dependence of the scattered intensity during polymerization.

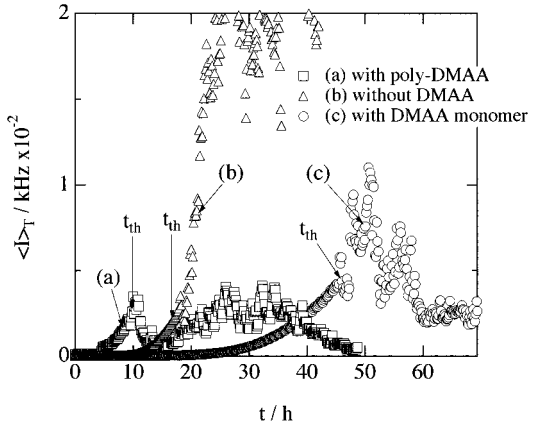

Figure 6. Scattered intensity, $\langle I \rangle_T$, variations during polymerization of TMOSs (a) in the presence of poly-DMAA, (b) in the absence of DMAA, and (c) in the presence of DMAA monomers.

First of all, the initial concentration dependence on gelation kinetics was examined. Figure 5 shows the monomer concentration dependence of the scattered intensity evolution of TMOS during polymerization. As shown in the figure, the gelation threshold t_{th} is not sensitive to the monomer concentration at all and is determined to be $t_{th} \approx$ 17 h.

Figure 6 shows the intensity variation during polymerization of TMOS (a) in the presence of poly-DMAA, (b) in the absence of DMAA, and (c) in the presence of DMAA monomer. The gelation process of TMOS was found to be strongly dependent on whether DMAA polymers/monomers are present or not in the reaction bath. In the presence of poly-DMAAs, the gelation was accelerated, while it was decelerated when DMAA monomers were present in the system, with respect to the case of TMOS without any additives. Another feature that can be drawn from the figure is that the peak intensity around gelation threshold seems to be depend on the architecture of DMAA. When poly-DMAAs exist, the concentration fluctuations of the system are highly suppressed. This is due to the fact that DMAA polymer chains filled in the reaction bath prevent TMOS clusters from evolution of their concentration fluctuations in the free space and allow to grow in a cage of entangled poly-DMAA chains. These phenomena were also seen in the poly(vinyl alcohol) system.[16]

A series of ICFs for the gelation process of TMOS/poly-DMAA are shown in Figure 7. A power-law behav-

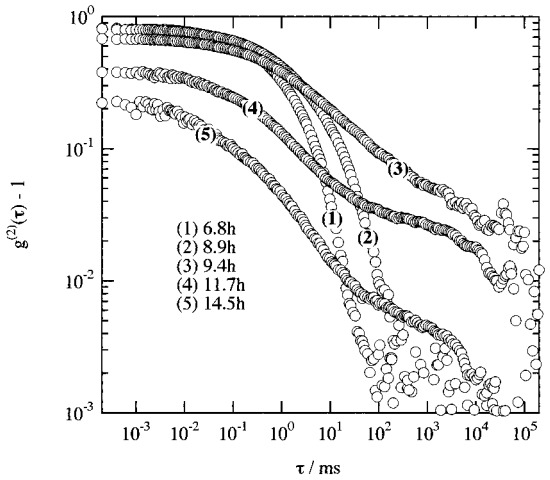

Figure 7. Double-logarithmic plots of the ICFs for TMOS/poly-DMAA system.

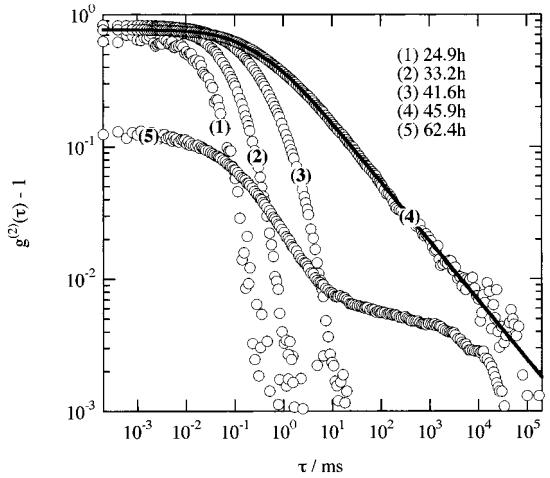

Figure 8. Double-logarithmic plots of the ICFs for TMOS/DMAA-monomer system.

ior appeared around $t \approx 9.4$ h, which is close to the time when $\langle I \rangle_T$ increased drastically (see Figure 6a). Furthermore, the initial amplitude of the ICF starts to decrease at the same time. Therefore, t_{th} can be determined to be around 9.4 h. Similarly, t_{th} for the TMOS/DMAA monomer system can be determined from Figure 8 to be about 45.9 h. The value of D_p was again 0.53 ± 0.1.

Now, we interpret the possible effects of DMAA on the gelation of TMOS. In the presence of DMAA monomers, active reaction sites of TMOS are capped with DMAA monomers by hydrogen bonding between the amide group in DMAA and the silanol group in TMOS (Figure 9). This interaction is also expected in the TMOS/poly-DMAA system. However, due to the existence of the connectivity of the polymer chain, the poly-DMAA chains play rather as a guide to coordinate TMOS monomers so as to react to the growing TMOS chains as shown in the figure. This is a kind of "cage effect", which results in an acceleration of the reaction of TMOS/poly-DMAA system.

The above conjecture can be supported by the following experimental results of gelation in the presence of inert component such as polystyrene or styrene monomers. The gelation process of TMOS/styrene hybrids was investigated to confirm the deceleration effect of DMAA monomers to the reaction of hybrid gel by the hydrogen bondings, of which results are shown in Figure

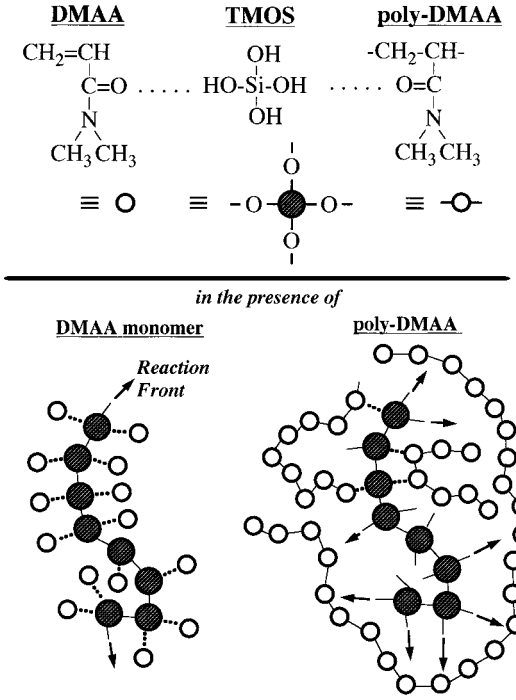

Figure 9. Schematic model showing hydrogen-bonding formation between silanol and amide groups in TMOS/DMAA monomer and TMOS/poly-DMAA hybrids. Open and hatched circles represent DMAA and TMOS monomer units, respectively. The dashed lines and arrows denote hydrogen bondings and continuity and/or reaction front of the TMOS chain, respectively. As depicted in this figure, poly-DMAA plays as a guide line for polymerization of TMOS and the polymerization is accelerated in the cage of a poly-DMAA chain ("cage effect").

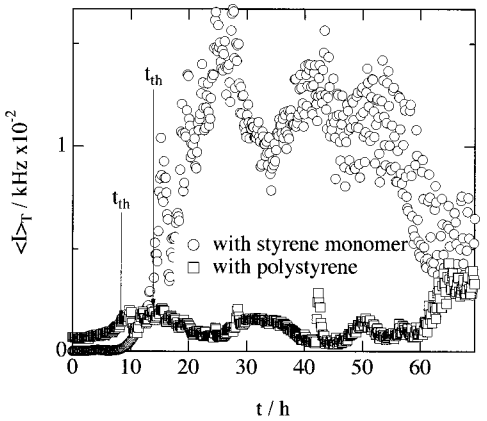

Figure 10. Scattered intensity, $\langle I \rangle_T$, variations during polymerization of TMOSs in the presence of styrene monomers (circles) and styrene polymers (squares).

10. The reactions are much accelerated in both cases where styrene monomers and polymers are present. However, the difference between TMOS with and without styrene monomers or polymers was not noticeable in this experiment.

On the basis of the experimental evidence disclosed in this work, we concluded that hydrogen bonding between the amide and silanol groups plays an important role in the gelation process of these hybrid gels. Brus reported in their NMR study that polyacrylate in the mixture not only acts as an inert filler but also affects the condensation kinetics and gels structure.[30] To our knowledge, however, there has been only a few reports about the effects of hydrogen bonding on the

kinetics of polymerization. Therefore, we believe that the finding of the opposite effects on polymerization kinetics of TMOS about the role of hydrogen bonding is of quite significance.

4. Conclusion

The gelation kinetics of organic−inorganic hybrid gels was characterized by TRDLS with four parameters, i.e., (1) the time-averaged scattered intensity, $\langle I \rangle_T$, (2) the time−intensity correlation function, ICF, (3) the distribution of the characteristic relaxation time, $P(\Gamma^{-1})$, and (4) the initial amplitude of the ICF, σ_I^2. During TRDLS experiments on the polymerization of TMOS, $\langle I \rangle_T$ dramatically increased at $t = t_{th}$, the time at which the gelation takes place. This drastic change in $\langle I \rangle_T$ is related to the power-law behavior in ICF, the significant broadening of $P(\Gamma^{-1})$, and the deviation of σ_I^2 from unity. These phenomena were explained as a result of restricted ergodicity of polymer gels and changes of spatial connectivity from finite to infinite connectivity.

The power-law behavior of ICF at the gelation threshold was characterized by the exponent D_p. The value of D_p was 0.53 ± 0.1 both for TMOS clusters and those in the presence of DMAA monomers. This indicates that the TMOS clusters studied in this work are highly screened by excluded volume, resulting in a deviation from the prediction for a percolation model for polydisperse clusters with the Fisher exponent τ_F of 2.25 and the fractal dimension $D = {}^5/_2$.

The gelation process of these polymer hybrids was found to be very sensitive to the organic component present in the reaction bath. In the presence of poly-DMAA, the gelation was accelerated, while in the presence of DMAA monomer, it was decelerated rather than silica gel. It was concluded that hydrogen bonding between the amide and silanol groups plays an important role in the gelation process of these polymer hybrids.

Acknowledgment. This work is partially supported by the Ministry of Education, Science, Sports and Culture, Japan (Grant-in-Aid, 09450362 and 10875199 to M.S.). Thanks are due to the Cosmetology Research Foundation, Tokyo, for financial assistance.

References and Notes

(1) Novak, B. M. *Adv. Mater.* **1993**, *5*, 422.
(2) Schubert, U.; Husing, N.; Lorenz, A. *Chem. Mater.* **1995**, *7*, 2010.
(3) Chujo, Y. *Polymeric Materials Encyclopedia;* Salamone, J. C., Ed.; CRC: Boca Raton, FL, 1996; Vol. 6, p 4793.
(4) Chujo, Y.; Saegusa, T. *Adv. Polym. Sci.* **1992**, *100*, 11.
(5) Saegusa, T. *J. Macromol. Sci., Chem. Ed.* **1990**, *A27*, 1603.
(6) Tamaki, R.; Naka, K.; Chujo, Y. *Polym. J.* **1998**, *30*, 60.
(7) Yoshida, M.; Prassad, P. N. *Appl. Opt.* **1996**, *35*, 1500.
(8) Dave, B. C.; Dunn, B.; Valentine, J. S.; Zink, J. I. *Anal. Chem.* **1994**, *66*, 1120.
(9) Winter, H. H.; Mours, M. *Adv. Polym. Sci.* **1997**, *134*, 167.
(10) Winter, H. H.; Chambon, F. *J. Rheol.***1986**, *30*, 367.
(11) Winter, H. H.; Morganelli, P.; Chambon, F. *Macromolecules* **1988**, *21*, 532.
(12) Martin, J. E.; Wilcoxon, J.; Adolf, D. *Phys. Rev. A.* **1987**, *36*, 1803.
(13) Martin, J. E.; Hurd, A. J. *J. Appl. Crystallogr.* **1987**, *20*, 61.
(14) Martin, J. E.; Wilcoxon, J. *Phys. Rev. Lett.* **1988**, *61*, 373.
(15) Martin, J. E.; Wilcoxon, J.; Odinek, J. *Phys. Rev. A* **1991**, *43*, 858.
(16) Norisuye, T.; Shibayama, M.; Tamaki, R.; Chujo, Y. *Polym. Prepr. Jpn.* **1998**, *47*, 904.
(17) Lang, P.; Burchard, W. *Macromolecules* **1991**, *24*, 814.
(18) Ren, S. Z.; Sorensen, C. M. *Phys. Rev. Lett.* **1993**, *70*, 1727.
(19) Pusey, P. N.; van Megen, W. *Physica A* **1989**, *157*, 705.
(20) Joosten, J. G. H.; McCarthy, J. L.; Pusey, P. N. *Macromolecules* **1991**, *24*, 6690.
(21) Shibayama, M. *Macromol. Chem. Phys.* **1998**, *199*, 1.
(22) Norisuye, T.; Shibayama, M.; Nomura, S. *Polymer* **1998**, *39*, 2769.
(23) Norisuye, T.; Takeda, M.; Shibayama, M. *Macromolecules* **1998**, *31*, 5316.
(24) Tanaka, T.; Hocker, L. O.; Benedek, G. B. *J. Chem. Phys.* **1973**, *59*, 5151.
(25) Daoud, M.; Martin, J. E. *Fractal Properties of Polymers*; Avnir, D., Ed.; John Wiley & Sons: New York, 1989; p 109.
(26) Adam, M.; Lairez, D. *Sol−Gel Transition*; Cohen Addad, J. P., Ed.; John Wiley & Sons: New York, 1996; p 87.
(27) Durand, D.; Delsanti, M.; Adam, M.; Luck, J. M. *Europhys. Lett.* **1987**, *3*, 297.
(28) Muthukumar, M. *Macromolecules* **1989**, *22*, 4656.
(29) Yamane, M.; Inoue, S.; Yasumori, A. *J. Noncryst. Solids* **1984**, *63*, 13.
(30) Brus, J.; Kotlik, P. *Chem. Mater.* **1996**, *8*, 2739.

MA981306H